Polymer Degradation and Stability 94 (2009) 1962–1971

Contents lists available at ScienceDirect

Polymer Degradation and Stability

journal homepage: www.elsevier.com/locate/polydegstab

Oxidation of a carbon/glass reinforced cyanate ester composite

Colomba Di Blasi [a,*], Carmen Branca [b], Antonio Galgano [a], Raffaela Moricone [a], Eva Milella [c]

[a] Dipartimento di Ingegneria Chimica, Università degli Studi di Napoli "Federico II", P.le V. Tecchio, 80125 Napoli, Italy
[b] Istituto di Ricerche sulla Combustione, C.N.R., P.le V. Tecchio, 80125 Napoli, Italy
[c] IMAST SCarl, P.le E. Fermi, Granatello, 80055 Portici, Italy

ARTICLE INFO

Article history:
Received 19 May 2009
Accepted 28 July 2009
Available online 3 August 2009

Keywords:
Fibre reinforced composite
Cyanate esters
Oxidation
Kinetics

ABSTRACT

The decomposition/oxidation behaviour of a carbon/glass fibre reinforced thermosetting pre-impregnated material based on polymerized aromatic cyanate ester compounds (commercial name GURIT-PN900-C582-43) has been investigated. Experiments were carried out for thermally thick samples exposed in a preheated reaction chamber (temperatures between 650–950 K) and a continuous gas flow (inlet velocity between 0.6 and 4.2 cm/s). Temperature measurements indicate that, in air, the process takes place under a mixed kinetic-diffusive control with three main dynamic stages corresponding to oxidative decomposition, heterogeneous ignition delay and oxidation. The oxidative decomposition stage is always much faster than the total duration of the ignition delay and oxidation stages (factors of 60–85). SEM pictures show dramatic changes in the material structure with amounts of solid residue, at the conclusion of the conversion process, varying from about 62% (resin char, glass and carbon fibres) to 29% (essentially the glass fibres) (against 85–75% for thermal degradation). Also, with the aid of thermogravimetric curves measured in air for the composite material and a charred residue, a three-step oxidation mechanism is proposed consisting of the oxidative decomposition of the resin, the oxidation of the resin char and the oxidation of the carbon fibres with estimated activation energies of 95, 136 and 185 kJ/mol, respectively.

1. Introduction

Fibre reinforced polymer composites are currently used in a variety of structural and thermal protection applications, including aerospace, marine, automotive, civil infrastructures, chemical processing, sporting goods and consumer products, owing to their many outstanding physical, thermal, chemical and mechanical properties [1]. These materials are usually made of glass, carbon, aramid or extended-chain polyethylene fibres with a polyester, vinyl ester, epoxy or phenolic resin matrix so that the poor resistance to fire and the high flammability are generally the main drawbacks [2]. Indeed, the material state and properties remain stable only for temperatures below the glass transition temperature [3]. For higher values, changes begin to occur and, with the activity of the decomposition and oxidation reactions, the material characteristics are profoundly modified. Furthermore, not only do the polymeric components and the combustible fibres undergo oxidation, so that all the active material is entirely consumed, but the glass reinforcement may also encounter serious deterioration. As a consequence, the thermally induced response of composite materials, as also demonstrated by numerous modelling studies [4–12], results from a very complicated interaction between chemical and physical processes and varies with the characteristics of the material properties and processing.

To investigate the mechanisms that control the conversion process, with the scope of improving the design of reliable and efficient thermal protection systems, in this study oxidation experiments have been made on a commercial material consisting of carbon and glass fibres impregnated with a thermosetting resin based on polymerized aromatic cyanate ester compounds. Polycyanurates are addition-cured thermoset polymers that find application in the manufacture of fibre-reinforced composites mainly for use in aircraft and printed circuits boards as well as adhesives and encapsulants [13]. The main paths of the thermal decomposition [14] and the standard flammability characteristics [13] of these resins have been investigated but the thermal behaviour, when used in composite systems, has not yet been given consideration. Also, no quantitative information is available on the oxidation kinetics needed to develop comprehensive predictive models. Therefore measurements of the oxidation characteristics of thermally thick samples were made to elucidate the role played by temperature and flow conditions on the thermal response of the composite material. Moreover, measurements of weight loss, for the conditions typical of thermal analysis, combined with

* Corresponding author. Tel.: +39 081 7682232; fax: +39 081 2391800.
E-mail address: diblasi@unina.it (C. Di Blasi).

0141-3910/$ – see front matter © 2009 Elsevier Ltd. All rights reserved.
doi:10.1016/j.polymdegradstab.2009.07.025

a numerical method of parameter estimation, are applied to formulate a multi-step oxidation mechanism and to evaluate the kinetic parameters.

2. Material and method

The material under study is a composite material developed by GURIT and denoted PN900-C582-43. It is a fibre reinforced thermosetting pre-impregnated material for aircraft interior parts. It consists of woven 50/50 hybrid fabric of 3 k HTA carbon fibre and E-glass filament yarn, 180 g/m^2, twill 2/2, pre-impregnated with 43% cyanate ester resin PN900 based on polymerized aromatic cyanate ester compounds. The pre-impregnated material is a non-porous laminate with a glass transition temperature of 503 K, especially suitable for aviation and aerospace industries, marine and automotive applications and machine industries.

A set of experimental tests was made to investigate the behaviour of the composite material when exposed in an oxidative or inert environment under known thermal and flow conditions. The main characteristics of the experimental system integrated by a data acquisition set, already used in previous investigations [15,16], and the sample can be seen in Fig. 1. Decomposition/oxidation of the sample (Fig. 1A) takes place in a steel reactor (Fig. 1B) (6.5 cm internal diameter and 45 cm length), where a forced flow is distributed through a perforated plate at the bottom. A radiant furnace is used to pre-heat both the reactor and the gas which is fed through a jacket (internal diameter 8.9 cm) at the reactor top. Temperature profiles along the reactor axis are measured by seven thermocouples (chromel-alumel type, 500 μm diameter), with their tips exiting from a protective steel tube, at chosen distances from the flow distributor. The lower reactor zone (about 15 cm) is isothermal at a temperature T_r, indicated in the following as heating temperature, determined by a proper selection of the furnace temperature (PID controller).

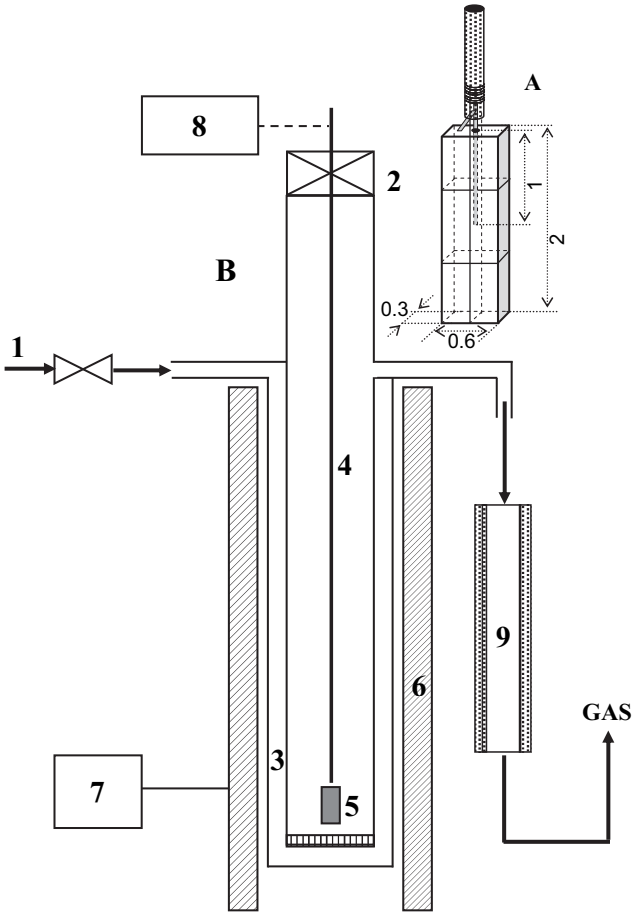

Fig. 1. Schematic of the sample (A, sizes in cm) and the reaction chamber (B): 1) gas feed, 2) isolating valve, 3) gas heating, 4) sample holder, 5) sample and thermocouples, 6) furnace, 7) controller, 8) acquisition data set, 9) hairpins.

Once the desired thermal conditions are achieved, the reactor closing cap is substituted by another one equipped with a thin steel rod acting as a support for the sample and the thermocouples, used to gain information about its thermal response. In this way, the sample is suspended in the preheated isothermal section of the reactor with the centre positioned along the axis at a distance of 3.5 cm from the flow distributor. It is heated by the hot gas flow and, mainly, by reactor wall radiation.

A 0.7 mm hole is drilled from the top to the centre of the composite material slab. It is used to locate a 0.5 mm sheathed type K thermocouple. Another thermocouple is located in close contact with the top surface of the sample. As already outlined, the two thermocouples are supported by a thin steel rod connected to the reactor cap. To minimize heat conduction rates, the thermocouples and the support are insulated by means of a ceramic tube and refractory cement. The sample is caged by a 300 mm Nichrome wire, tied to the steel rod, to permit a direct exposition to radiative and convective heating.

After the sample centre reaches the heating temperature or higher values, the furnace is kept at the set point for 30–120 min, depending on the heating conditions, then the power is turned off. The sample is left under a forced gas flow until the temperatures lowers to 450 K, then it is collected to evaluate the characteristics of the solid residue also by means of Scanning Electron Microscope (SEM) analysis.

Thermogravimetric experiments have also been carried out of the composite material and residues collected from the experiments described above, preliminarily reduced to small sized particles. The experimental system has been already presented elsewhere [15,17–20] and only the main characteristics are discussed here. It consists of a furnace, a quartz reactor, a PID controller, a gas feeding system, an acquisition data set, and a precision balance. The furnace is a radiant chamber, which creates a uniformly heated zone, where a quartz reactor is located. The sample is exposed to thermal radiation by means of a stainless steel mesh screen, whose sides are wrapped on two stainless steel rods connected to a precision (0.1 mg) balance, which allows the weight of the sample to be continuously recorded. An air flow establishes the proper reaction environment. Solid conversion occurs under known thermal conditions by means of feedback control of the sample temperature (measured by a close-coupled thin thermocouple), using the intensity of the applied radiative heat flux as the adjustable variable.

3. Results

In this section results are presented first of the characteristics of the thermal response of thick samples exposed in a preheated reaction chamber under a forced flow of air or nitrogen. The thermal history undergone by the sample is useful to evaluate the heating rate, the reaction temperatures and the burning/decomposition times. The solid residues collected at the conclusion of the conversion process are used to evaluate the chemico-physical changes induced in the sample structure by the thermal treatment. Then, the thermogravimetric behaviour of the composite material and residues left from the previous set of experiments is investigated. Finally, with the analysis of the experimental results, a multi-step mechanism is proposed for the oxidation of the fibre reinforced polymer composite under study.

3.1. Thermal response of the composite material under heat and mass transfer control

Experiments with thermally thick samples of the composite material have been carried out in air for heating temperatures, T_r, between 650 and 950 K and an inlet gas velocity, u, of 0.6 cm/s and for a heating temperature of 900 K as the inlet gas velocity was varied in the range 0.6–4.2 cm/s. Also a few tests have been carried out in nitrogen (inlet gas velocity 0.6 cm/s) again for heating temperatures between 650 and 950 K. The maximum heating temperature, also taking into account the heat released from the oxidation, causes the complete conversion of the active part of the composite material with small modifications of the glass fibres. Samples were cut in the form of parallelepipeds 0.3 cm thick, 0.5 cm wide and 2 cm long with the internal and external thermocouples positioned as in the schematic of Fig. 1A. Each experiment was repeated from three to five times.

An example of the heating dynamics of the material in air and nitrogen ($u = 0.6$ cm/s) is shown in Fig. 2 for $T_r = 750$ K, by means of the profiles of the internal and surface temperatures, T_i and T_e. The two temperature profiles are similar but T_i always shows higher values. Given the small size (and mass) of the sample, the dynamics of the surface thermocouple are essentially determined only by the conditions of the forced flow and the effects of the mixing between the imposed flow and the flow of decomposition/oxidation products. Indeed, in the case of air flow, the extremely lean fuel mixture does not allow the proper conditions to be established for homogeneous gas-phase reactions. The higher T_i values can be, in the first place, explained by the more important role played by radiation from the reactor walls with respect to convective heating of the sample. Moreover, in the presence of air, the walls of the hole, where the thermocouple is allocated, create a confined narrow zone where the exothermic character of the reaction of solid conversion dominates the characteristics of the imposed flow. As long as the temperature remains below approximately 700 K, the profiles measured in nitrogen and air are practically coincident, indicating that there are no detectable changes in the energetic character of the decomposition reactions that are likely to be active for temperatures above the glass transition temperature of the polymeric resin (503 K). Then, in nitrogen, there is a tendency for the internal and external temperature to become coincident and to remain at constant values below the external heating temperature for long times. In air, the exothermicity of the heterogeneous reactions of the solid phase initially causes a slow continuous increase in the temperature, that can be interpreted as an ignition delay or an induction period. This is followed by the occurrence of heterogeneous ignition of the solid with a significant activity of solid-phase oxidation reactions as testified by the attainment of maximum T_e values of about 875 K. Finally a rapid decline towards the external heating value is observed as a consequence of either the lack of adequate conditions (temperature, concentration and/or availability of oxygen and combustible solid material) for the progress of the reaction or the complete depletion of the active part of the composite material.

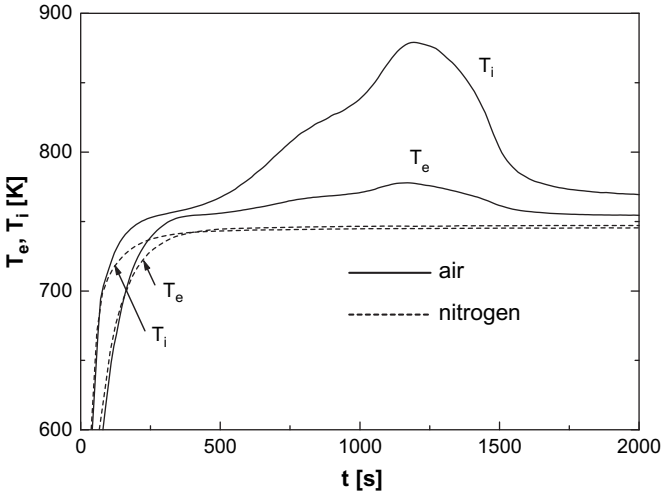

Fig. 2. Time profiles of the internal (T_i) and external temperature (T_e), as measured in air (solid lines) and nitrogen (dashed lines) for a heating temperature, T_r, of 750 K and an inlet gas velocity, u, of 0.6 cm/s.

Given the weak energetic character of the thermal decomposition reactions (and the coincidence of the measured temperature profiles in air and nitrogen for low temperatures, also for high T_r values), the analysis of the temperature profiles to get information about the characteristic times/temperatures of solid conversion mainly considers the measurements in air. The thermal decomposition experiments are useful to evaluate the amount of char produced from the thermal decomposition of the polymeric resin and to observe the changes induced by the reactions on the material structure. Moreover, given the same qualitative shape of the T_e and T_i profiles, the analysis is limited to T_i. The case of a heating temperature equal to 750 K and an air inlet velocity of 0.6 cm/s is chosen to introduce the characteristic parameters as, on one side, this temperature is sufficiently high for the activity of oxidative/thermal decomposition and oxidation reactions and, on the other, it is still low to permit a good resolution between the different process stages. Fig. 3A–B report the T_i profiles and the corresponding time derivatives dT_i/dt and d^2T_i/dt^2 over the time interval 0–100 s and 0–2000 s, respectively. It appears (Fig. 3A) that, after a very rapid temperature rise, the heating rate is reduced not only for the approach to the heating temperature but probably also for the convective cooling associated with the flow of volatile products and the endothermicity of oxidative decomposition reactions. A time, t_{hm}, with the corresponding maximum heating rate, h_m and a time, t_g, when the glass transition temperature, T_g, is achieved can be easily identified from Fig. 3A. Moreover, a time, t_d, and a temperature, T_d, are also defined corresponding to the conclusion of the decomposition stage, assumed to coincide with the second local maximum in d^2T_i/dt^2. Thus, the decomposition period is $\Delta t_d = t_d - t_g$. Fig. 3B shows the other two main stages of the process, that is, that corresponding to the induction period, Δt_{id}, and that of strong oxidation, Δt_o, as testified by the wide region of temperatures above the heating temperature. More precisely, the ignition delay time (or induction time), t_{id}, and the corresponding temperature, T_{id}, are assumed to coincide with the second local maximum in dT_i/dt whereas the conclusion of the conversion process, t_c, and corresponding temperature, T_c, are assumed to coincide with the last local maximum in d^2T_i/dt^2 (Fig. 3B). Hence, the induction period is $\Delta t_{id} = t_{id} - t_d$ and the oxidation period is $\Delta t_o = t_c - t_{id}$. Fig. 3B also shows the maximum temperature, T_{max}, and the corresponding time, t_{max}, which represent the conditions of maximum activity of the heterogeneous oxidation reactions. Finally, the amounts of solid residues are evaluated with reference to the initial mass sample for the experiments carried out in nitrogen (Y_{rd}) and air (Y_{ro}).

The parameters, introduced through Fig. 3A–B, are obtained from various measurements and reported versus the heating temperature in Fig. 4 (t_g, T_d, t_d, h_m), Fig. 5 (T_{id}, t_{id}, Y_{ro}, Y_{rd}) and Fig. 6 (T_{max}, t_{max}, T_c, t_c) for the case of $u = 0.6$ cm/s. Examples of the measured T_i versus time profiles for various T_r are shown in Fig. 7. In all cases, the maximum heating rate, h_m, is achieved at very short times, before the attainment of the glass transition temperature. It becomes successively higher and shows a linear dependence on

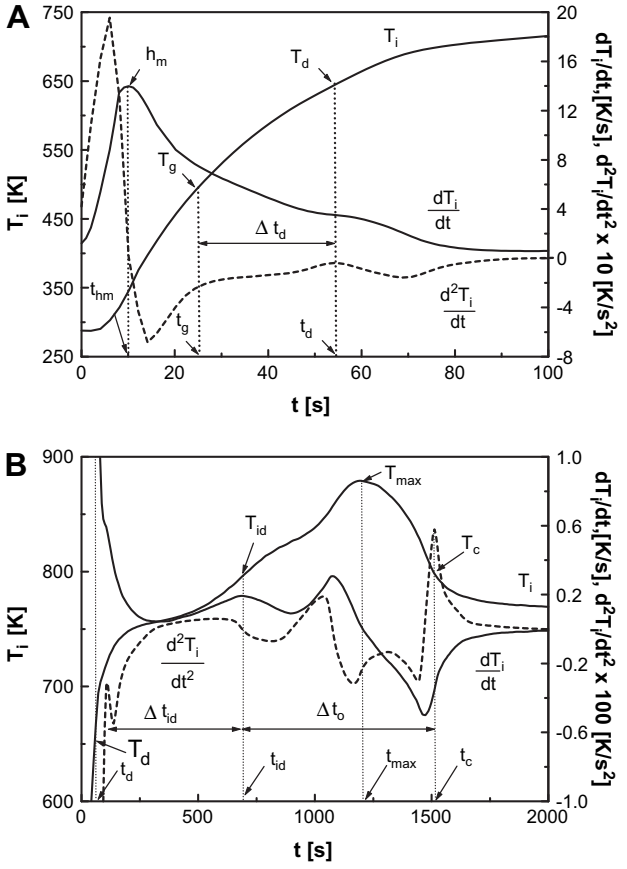

Fig. 3. Time profiles of the internal temperature (T_i) and the time derivatives dT_i/dt and d^2T_i/dt^2, over the interval 0–100 s (A) and 0–2000 s (B) (T_r = 750 K and u = 0.6 cm/s) with the definition of the process parameters: maximum heating rate, h_m, and corresponding time, t_{hm}, glass transition temperature, T_g, and corresponding time, t_g, decomposition temperature, T_d, and corresponding time, t_d, ignition delay time, t_{id}, and corresponding temperature, T_{id}, maximum temperature, T_{max}, and corresponding time, t_{max}, conversion time, t_c, and corresponding temperature, T_c, decomposition period, $\Delta t_d = t_d - t_g$, induction period, $\Delta t_{id} = t_{id} - t_d$, and oxidation period, $\Delta t_o = t_c - t_{id}$.

T_r with values roughly comprised between 9 and 26 K/s. The time needed to achieve the glass transition temperature is also rather short and decreases as T_r is increased (from about 40 to 14 s). It is indicative of the duration of the initial (inert) heating stage. Then, reactions begin that concern oxidative decomposition and oxidation of the active solid. Decomposition reactions, even though the

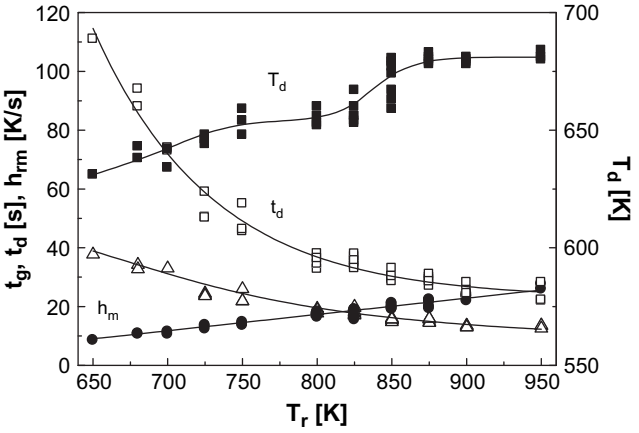

Fig. 4. Maximum heating rate, h_m, characteristic times, t_g and t_d, and decomposition temperature, T_d, versus the heating temperature for an inlet air velocity of 0.6 cm/s.

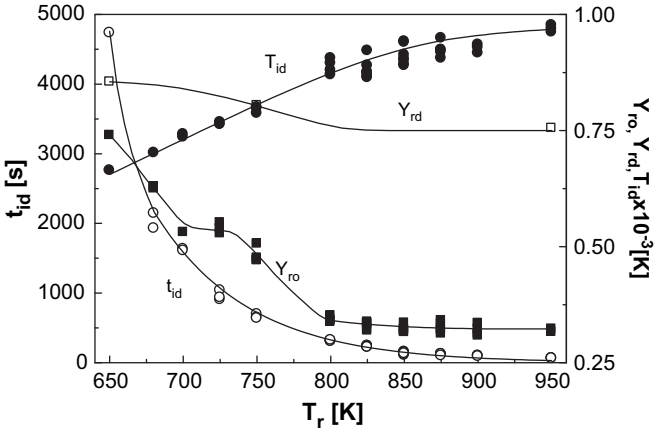

Fig. 5. Ignition delay time, t_{id}, and corresponding temperature, T_{id}, and yields of solid residues collected at the conclusion of the experiments, Y_{ro}, versus the heating temperature, T_r, for an inlet air velocity of 0.6 cm/s. The solid residue yield obtained from experiments carried out in nitrogen and the same inlet gas velocity, Y_{rd}, is also reported.

presence of oxygen may play a role, are essentially volumetric thermally driven reactions [21]. Conversion of solid fuels in oxidizing or reducing environments is much more complicated as it results from several processes, such as [22]: 1) film diffusion of oxidizing/gasifying agent, 2) diffusion through the layer of inert unreacted material and the sample, 3) adsorption onto the reaction surface, 4) chemical reaction, 5) desorption of product gas from the surface, 6) diffusion of product gas through the sample and the inert layer, 7) film diffusion back into the ambient gas. Apart from the surface chemical reaction, the remaining are mass-transport steps. A chemical control is generally established only for low temperatures and samples so small that the diffusion rate is much faster than the chemical reaction rate. For the size of the samples and heating temperatures examined here it is likely that the rate of gaseous species diffusion towards the reaction zone is comparable to the reaction rate, leading to a limited penetration of the gas in the solid so that the reaction mainly occurs across the external sample surface. The examination of the characteristic times and temperatures on dependence of the heating temperature for a low inlet air velocity (0.6 cm/s) permits the identification of two main modes of solid oxidation (it is worth recalling that it is appropriate to consider the process under study as solid oxidation given that the external temperature is always lower), characterized by a single ignition or distributed ignitions over the sample surface, respectively.

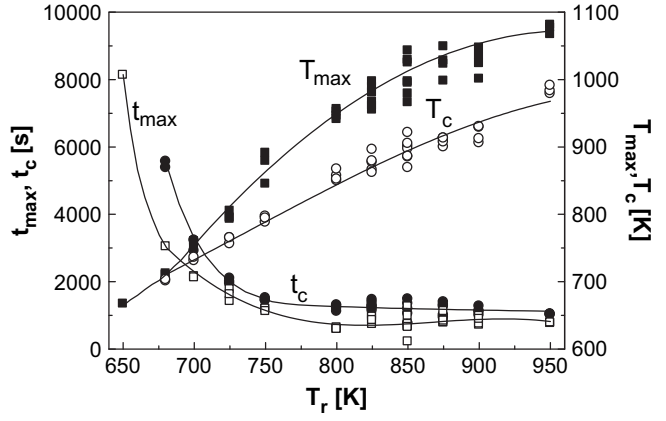

Fig. 6. Maximum temperature, T_{max}, and corresponding time, t_{max}, and conversion time, t_c, and corresponding temperature, T_c, versus the heating temperature, T_r, for an inlet air velocity of 0.6 cm/s.

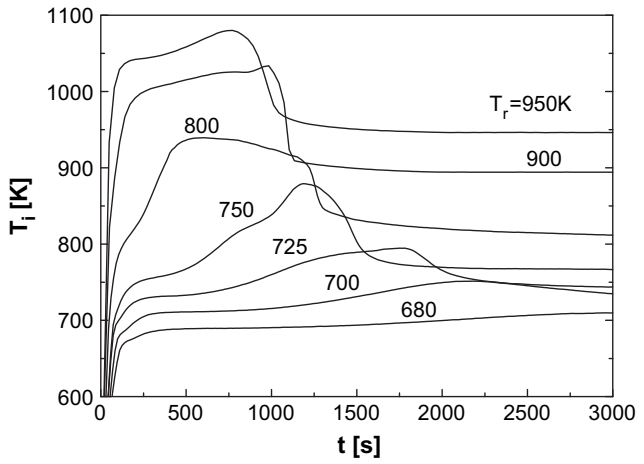

Fig. 7. Time profiles of the internal temperature as measured for several heating temperatures, T_r, and an inlet air velocity of 0.6 cm/s.

The first mode of solid oxidation is observed for a T_r range of 650–800 K. The decomposition temperature T_d is not significantly affected by the external heating conditions (630–655 K) with the duration of the decomposition process, Δt_d, varying from about 75 to 17 s. On the other hand, the time t_{id} presents a zone of rapid decrease (with Δt_{id} from about 4600 s to 290 s) accompanied by a significant increase in T_{id} (from about 660 to 870 K). The maximum temperature, T_{max}, continuously increase with variations with respect to the heating temperature from about 14 K ($T_r = 680$ K) to150 K ($T_r = 800$ K) while the characteristic times of the oxidation period, t_{max} and t_c, are progressively reduced ($\Delta t_o = 3400$–900 s, the lower limit refer to $T_r = 680$ K as for lower values it is not possible to exactly define the conclusion of the conversion process). Also, from the measured amounts of solid residue (Fig. 5) and taking into account a contribution of 28.5% of glass fibres, it appears that the active material has been almost completely consumed.

The decomposition reactions take place at much lower temperatures and are faster than the oxidation reactions (the total time period needed for the oxidation is actually $\Delta t_{id} + \Delta t_o$ which is much longer than Δt_d). Moreover, not only the ratio $\Delta t_o/\Delta t_d$ is high (65–53) but also Δt_{id} is significantly longer than Δt_d (factors of 40–17), so that oxidative decomposition and oxidation are essentially sequential processes. The relatively mild external heating conditions and the rather long induction times most likely lead to an almost uniform distribution of the sample temperature. This is accompanied by a very intense activity of the oxidation reactions over the entire sample volume causing a single zone (the entire sample surface) of heterogeneous ignition and oxidation. Indeed a continuous increase in the sample temperature with a maximum deviation with respect to the heating temperature of about 150 K and the complete depletion of the active material are observed. At these relatively mild heating conditions, it can be postulated that the control of the process is mainly of kinetic (thermal) type.

A single ignition/oxidation zone is also observed for high heating temperatures (T_r greater or equal to 875 K) with the characteristic temperatures of the process, T_d, T_{id} and T_{max}, approaching constant values (about 680, 950, 1050 K, respectively) while the T_c values still present continuously increasing values as they are determined mainly by the imposed heating (Figs. 4–6). The duration of the decomposition period remains approximately constant around 15 s, although the high T_d values suggest that some overlap occurs between this reaction stage and the highly exothermic oxidation reactions. Furthermore, the total duration of the oxidation dynamics also show small variations. The severe heat fluxes, associated with high T_r values, cause a rapid heating of the entire external surface of the sample, the ignition delay becomes very short and heterogeneous ignition/oxidation concerns the entire sample surface. However, the weak influence of the heating temperature on the oxidation characteristics indicates that, when heating conditions are severe, the control of the oxidation process shifts to oxygen diffusion. It is worth recalling that, in addition to the active surface, the global oxidation rates also include dependences of the Arrhenius type on the temperature and a power-law type on the oxygen partial pressure [22].

For both low and high heating temperatures, the temperature measurements show a good reproducibility and the uncertainty in the estimated parameters is small. Instead, for intermediate heating temperatures (875 K $> T_r >$ 800 K) the scatter in the experimental data becomes significant although, on the average, the characteristic times and temperatures show values that link up well with those of the low and high T_r ranges. In reality, as the heating temperature is increased, heterogeneous ignition and oxidation are not any longer occurring along the entire sample surface. The spatial gradients across the sample volume increase while the still relatively mild heating conditions do not permit the attainment of an almost uniform surface temperature at the ignition time. Also, for this set of experiments, the air flow rate is slow and so is the oxygen partial pressure. In this way, heterogeneous ignition is a local process whose location is not exactly reproduced by each experiment. Hence, this peculiar ignition mode is responsible for the larger scatter in the process parameters which are evaluated only by means of the recorded temperature at the sample centre.

The analysis of the temperature measurements integrated by the yield curves of the solid residues (Y_{ro} and Y_{rd}, Fig. 5) and SEM photographs (8A–8H) also permits to understand the details of the oxidation process. The composite material in its original form reveals the presence of the reinforcing fibres that are embedded within the polymeric resin (Fig. 8A, view of the sample thickness). As the material consists of layers of interwoven glass and carbon fibres, Fig. 8A shows alternately their cross and longitudinal views. In particular, a magnified view (Fig. 8B) makes visible a series of parallel furrows, along the lateral surface of the carbon fibres.

The yields of the solid residues collected from sample conversion in nitrogen are quantitatively different from those obtained from oxidation (air) experiments even at very low heating temperatures, indicating that the reaction paths (and the amount of char associated with the resin transformation) are affected by the reaction environment. For decomposition in nitrogen, the amount of solid collected varies from 85.5% ($T_r = 650$ K) to 75% ($T_r = 950$ K) which, taking into account a contribution of 28.5% for both the glass and carbon fibres, correspond to char yields generated from resin decomposition of 28.5 and 18% on a total mass basis (66.3 and 42% on resin mass basis).

Char yields from the thermal decomposition of nine cyanate ester monomers with different chemical structure have been determined [14] for the conditions of thermal analysis (5 K/min up to 1173 K). They vary in the range 31–63%, are sensitive to the chemical structure of the monomer and increase with the glass transition temperature. The yield reported for one of the polycyanurates (XU-71787) carrying a glass transition temperature of 517 K (versus 503 K of the material under study) is 33% which is lower than the lowest figure found here (42% on a resin mass basis for a heating temperature of 950 K). However, apart from the differences in the thermal conditions, the resin of interest here is not a monomer but a mixture of aromatic cyanate ester compounds.

As a consequence of volatile release caused by thermal decomposition, the reinforcing fibres and the interwoven structure of the composite become more clearly visible as can be observed from Fig. 8C ($T_r = 950$ K) when compared with the unreacted material (Fig. 8A). A magnified view (not shown) reveals that the

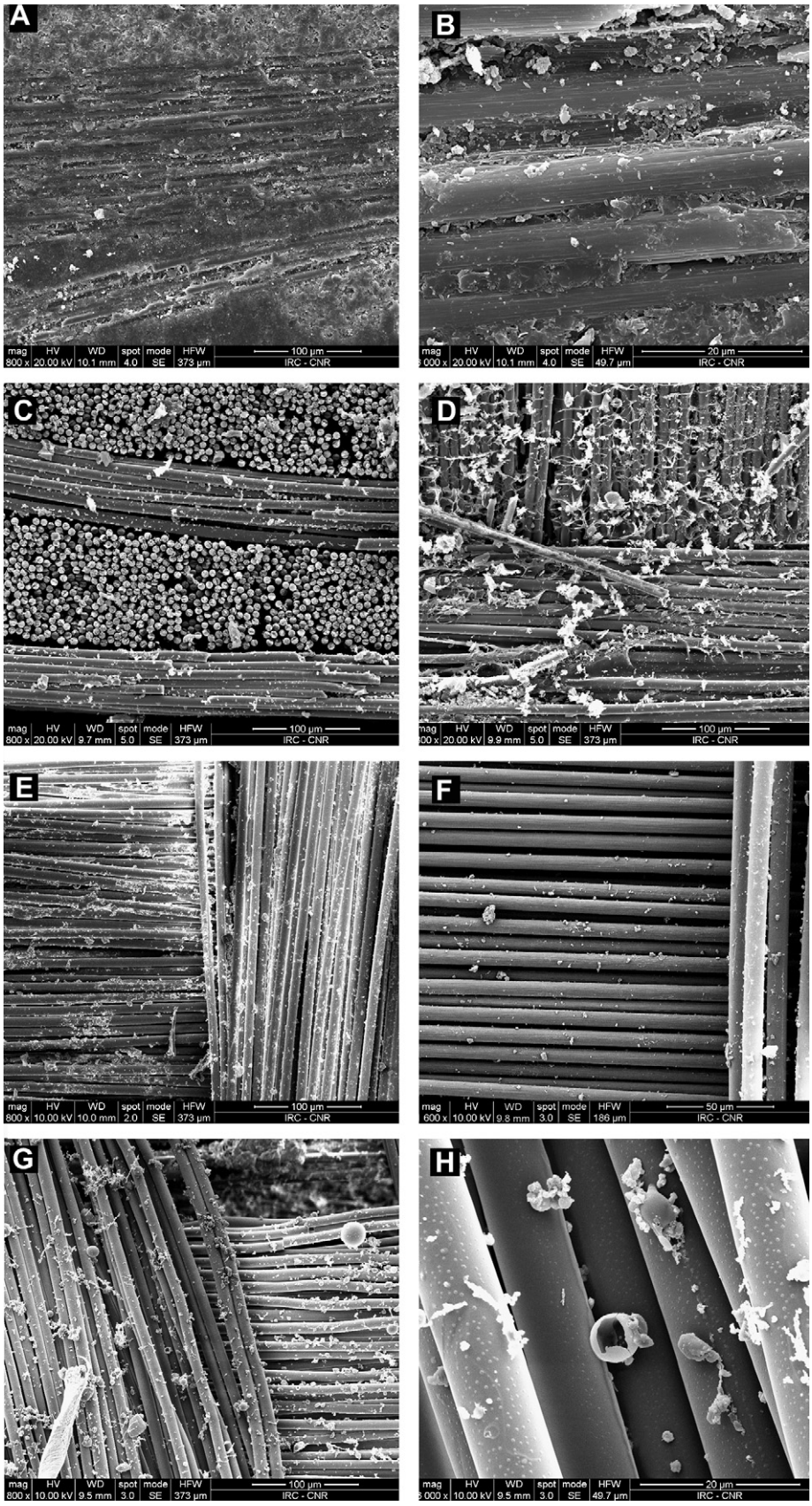

Fig. 8. SEM pictures of the composite material (A,B: views of the sample thickness), the residue from an experiment at $T_r = 950$ K in nitrogen (C: sample thickness, D: internal cross section), the residue from an experiment at $T_r = 700$ K in air (E, F: internal cross section) and the residue from an experiment at $T_r = 900$ K in air (G,H: internal cross section) (inlet gas velocity always equal to 0.6 cm/s).

smooth glass fibres with a diameter of 10 μm are in the horizontal position whereas those showing a cross section diameter of about 6 μm are the carbon fibres. The internal layers of decomposed material, as for instance those of Fig. 8D, show that the char occupies only partially the volume initially filled in by the virgin resin, so that the surface of the reinforcing fibres are for a large part exposed to heat/oxygen attack.

In air, for heating temperatures of 650–680 K (corresponding to T_{max} below 710 K), the reinforcement of the composite appears to be unaltered while partial oxidation of the resin char has occurred (residues are about 74–62% of the initial sample mass). The qualitative characteristics of the residues are the same as already discussed for thermal decomposition. For heating temperatures between 700 and 725 K (and T_{max} values of 760–800 K), the residue, about 53%, is mainly made of the glass and carbon fibres. SEM pictures of an internal layer of the residue (Fig. 8E–F, carbon and glass fibres are in a horizontal and vertical position, respectively) clearly shows that the resin char is noticeably reduced when compared with the case of thermal decomposition (Fig. 8D). Oxidation of the carbon fibres takes place at a successively larger extent until for T_r above 800 K, apart from very small quantities, the residue is made only by the glass fibres. SEM pictures, as shown by Fig. 8G–H ($T_r = 900$ K and T_{max} around 1050 K), confirm this finding and also indicate that the modifications at the surface of the glass fibres, barely visible for the experiments carried out at lower temperatures (Fig. 8D–F), are much more significant and evidenced by the formation of an extended network of bubbles.

It can be speculated that the heterogeneous reactions occur at the sample surface and, in the first place, regard the polymeric resin in its original or charred form also because the carbon fibres are, for a large part, not accessible. Once the polymeric component is depleted, the carbon fibres are attacked with the glass fibres acting as a physical barrier against oxygen diffusion. In other words, it is not only the intrinsic reactivity of the various components but also the structure of the material that determines which part of the material undergoes first to heterogeneous oxidation.

Examples of measurements, made to investigate the role played by oxygen diffusion on the burning characteristics are shown in Fig. 9 for a high heating temperature ($T_r = 900$ K). Some of the parameters, as defined in Fig. 3A–B, are reported on dependence of the inlet air velocity in Fig. 10. The main result obtained from this set of experiments is that increasing the rate of oxygen supply enhances solid conversion, more specifically the rates of the oxidation reactions. For the range of flow rates examined, the variations on the decomposition and induction parameters are

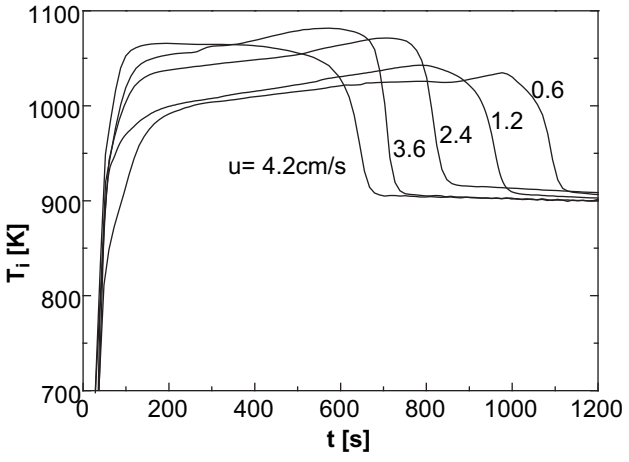

Fig. 9. Time profiles of the internal temperature as measured for several inlet air velocities and a heating temperature, T_r, of 900 K.

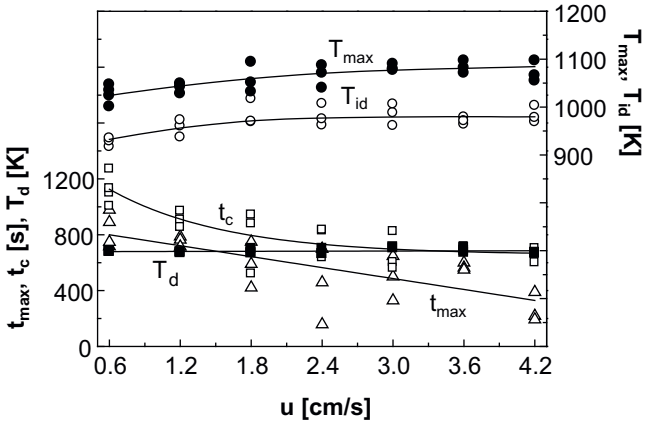

Fig. 10. Characteristic temperatures (T_d, T_{id} and T_{max}) and times (t_{max}, t_c) versus the inlet air velocity, u, for a heating temperature, T_r, of 900 K.

small (T_d and T_{id} values comprised between 680–685 K and 930–980 K, Δt_d around 15 s and Δt_{id} between 80–50 s). Instead, the maximum deviation of the temperature with respect to the heating temperature becomes rather large (from 125 to about 180 K) with a diminution in the oxidation period from about 1030 to 600 s. In other words, even at high heating (and reaction) temperatures, the oxidation process can be further enhanced, provided successively higher oxygen partial pressures.

3.2. Weight loss characteristics and oxidation kinetics

As can be inferred form the analysis of the experiments carried out for thermally thick samples, the peculiar structure of the composite material under study and the presence of the glass fibres can represent significant obstacles to gaseous reagent transport towards the reaction zones. Hence a rigorous theoretical approach, to investigate the oxidation kinetics, would require the formulation of advanced models including a detailed description of both chemical and physical processes, as the thermal response of the material is the result of interaction between the two [12]. A correct treatment for kinetic modelling could be based on separate analysis of a) the oxidative decomposition kinetics of the polymeric resin, b) the oxidation kinetics of the resulting char and the c) oxidation kinetics of the carbon fibres, using experiments carried out under a pure kinetic control. As the components are not generally available for commercial materials, the investigation is limited to the composite material and a charred residue using conversion conditions that minimize heat and mass transfer limitations (small sample mass, small particle sizes, slow heating rates and high air flow rates). The residue is collected from the oxidation of a thick sample exposed at a heating temperature of 700 K and an inlet air velocity of 0.6 cm/s, resulting in a maximum sample temperature of 750 K. The residue amounts to 53% and SEM pictures (Fig. 8E–F) show that a large part of the sample is made of carbon fibres. Moreover, in this case, before the thermogravimetric experiments, the glass fibres have been preliminarily removed. Experiments have been made with a mono-particle layer (particle sizes below 240 μm) for a total mass of 4 mg. The sample has been heated at 5, 7.5 and 10 K/min up to a final temperature 1000 K under a nominal air velocity of 0.5 cm/s. Each thermogravimetric test has been made in triplicate, showing good reproducibility.

Based on the results of the experiments carried out under heat and mass transfer control and the measured thermogravimetric curves, it appears that at least three main reaction stages should be modelled taking into account oxidative decomposition of the resin

(k_1,k_4), oxidation of the resin char (k_2) and oxidation of the carbon fibres (k_3) as in the following conceptual reaction mechanism:

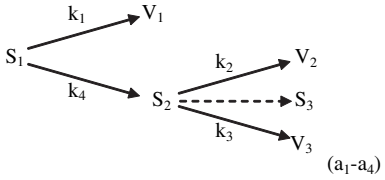

where S_1 is the composite material, V_1, V_2 and V_3 lumped volatile products (generated from oxidative decomposition of the resin, oxidation of the resin char and oxidation of the carbon fibres, respectively), S_2 a solid-phase reaction intermediate made of resin char and carbon and glass fibres, and S_3 the final residue made of glass fibres.

In reality, as well known from the previous literature on both decomposition [21] and oxidation [22] kinetics of solid fuels, thermogravimetric measurements only permit the evaluation of the rates of volatile formation from the various reaction steps. For this purpose, the application of kinetic models based on parallel reactions appears to be more general as it may more easily take into account the possible overlap among the reaction steps. Thus a set of three and two independent parallel reactions is considered for the composite S_1 and the residue S_2, respectively:

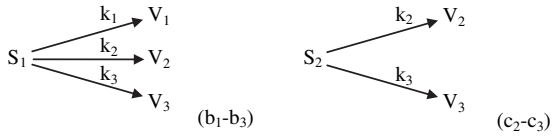

Symbols are the same as in the mechanism a1–a4. The meaning and values of kinetic constants k_1–k_3 are also the same in the mechanisms a1–a4, b1–b3 and c2–c3. For the residue S_2 (reactions c2–c3), the first reaction step is absent as the decomposition process has already occurred.

The reactions rates present the usual Arrhenius dependence (A_i are the pre-exponential factors and E_i the activation energies) on the temperature and a power law (n_i) dependence on the solid mass fraction. This treatment is more general than the first-order linear rates of the decomposition reactions and, at the same time, effectively takes into account the evolution of the pore surface area during char or carbon oxidation [15,17,22]. As in previous studies [15,17–20], for the stage of char oxidation, given that the dependence of the oxidation rate on the oxygen concentration is not investigated and the oxygen partial pressure is at constant value of air, its contribution is incorporated in the pre-exponential factors. Since the sample temperature, T, is a known function of time ($T = T_0 + ht$, T_0 is the initial temperature and h is the heating rate), the mathematical model consists of three (S_1) or two (S_2) ordinary differential equations for the mass fractions, Y_i, of the lumped classes of volatiles generated:

$$\frac{dY_i}{dt} = -A_i \exp(-E_i/RT) Y_i^{ni} \quad Y_i(0) = \nu_i \quad i = 1,3$$

where ν_i, indicated in the following as stoichiometric coefficients, are the initial mass fractions of the volatile products to be released. The parameters to be estimated are the activation energies (E_1–E_3), the pre-exponential factors (A_1–A_3), the reaction orders (n_1–n_3) and the stoichiometric coefficients (ν_1–ν_3). The kinetic parameters are estimated through the numerical solution (implicit Euler method) of the mass conservation equations and the application of a direct method for the minimization of the objective function, which considers both integral (TG) and differential (DTG) data, following a method already described [15,17]. The simultaneous use of experimental data measured for several heating rates avoids possible compensation effects in the kinetic parameters. The optimization procedure has been executed by requiring the same values of the activation energies, pre-exponential factors and exponents for all the curves. Moreover, given the narrow range of heating rates examined, constant (average) values have also been considered for the stoichiometric coefficients.

Deviations of the simulated versus the measured curves are computed as [17]:

$$\%\text{dev} = \frac{\sqrt{S/N}}{(\Phi_i)_{\text{exp,peak}}} \times 100, \quad S = \sum_{i=1,N} \left[(\Phi_i)_{\text{exp}} - (\Phi_i)_{\text{sim}}\right]^2 \tag{1–2}$$

where i represents the measured (exp) or simulated (sim) variable, Φ is the solid mass fraction, Y, or the rate of volatile product release, $-dY/dt$, at the time t, N is the number of experimental points and the subscript "peak" indicates the maximum value. Average values are considered below of the stoichiometric coefficients for the three different heating rates examined.

A comparison between the model predictions and the measurements is shown in Fig. 11A–B for the case of a heating rate of 5 K/min including the imposed heating profile to facilitate the definition of the temperature ranges of interest for the reaction

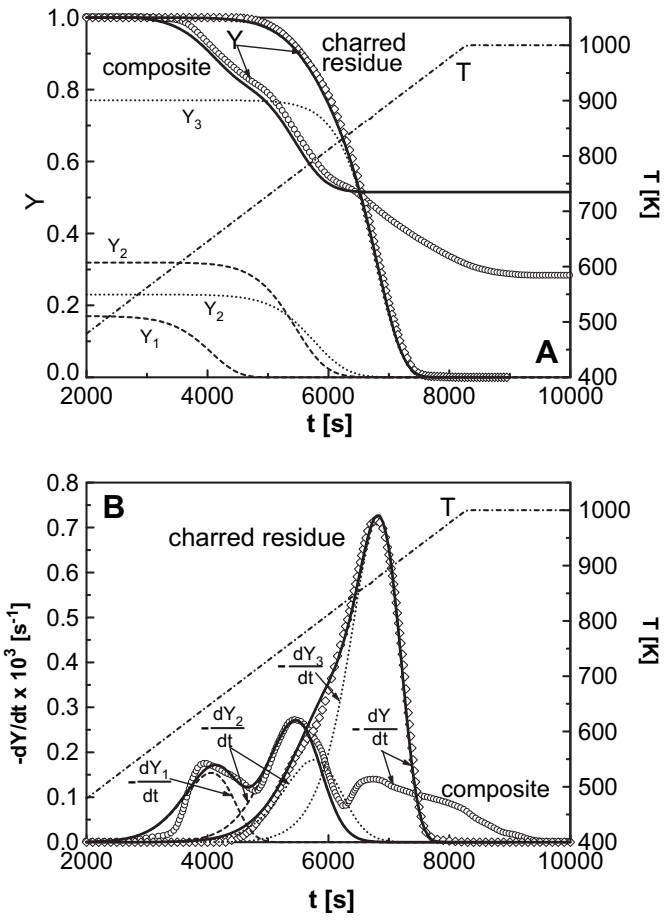

Fig. 11. A–B – Measured (symbols) and predicted (solid lines) mass fractions (A) and time derivatives of the mass fractions (B) of the composite and the charred residue ($T_r = 700$ K, $u = 0.6$ cm/s in air) versus time for thermogravimetric analysis conditions (heating rate of 5 K/min up to 1000 K). Predicted mass fractions (A) and time derivatives of the mass fractions (B) of the three volatile mass fractions are also reported for the composite (dashed lines) and the charred residue (dotted lines).

Table 1
Kinetic parameters for the three-step oxidation mechanism (pre-exponential factor, A, activation energy, E, exponent of the solid mass fraction, n, stoichiometric coefficient, ν) consisting of oxidative decomposition (A_1, E_1, ν_1), oxidation of the resin char (A_2, E_2, n_2, ν_2) and oxidation of the carbon fibres (A_3, E_3, n_3, ν_3) and percentage deviations, dev, between predictions and measurements for the integral (TG) and differential (DTG) data.

	Composite material	Charred residue
E_1 [kJ/mol]	94.5	–
A_1 [s^{-1}]	8.5×10^4	–
E_2 [kJ/mol]	136.0	136.0
n_1	1.00	
A_2 [s^{-1}]	5.0×10^6	2.5×10^6
n_2	1.20	1.20
E_3 [kJ/mol]	–	185.0
A_3 [s^{-1}]	–	2.2×10^8
n_3	–	1.00
ν_1	0.17	–
ν_2	0.31	0.23
ν_3	–	0.77
devTG%	2.05	0.98
devDTG%	4.90	1.51

steps. Estimated kinetic parameters and deviations are listed in Table 1. It can be observed that the composite material begins to lose weight at about 550 K. For the temperature range 550–775 K, the differential curve shows the presence of two well defined peaks, attributed to oxidative decomposition of the polymeric resin and oxidation of the resin char, respectively. The estimated values of the activation energies are about 95 and 136 kJ/mol, respectively, with amounts of volatiles released by the two reaction steps of 17 and 31%. For these two reaction steps, the agreement between predictions and measurements is acceptable (deviations between 2 and 5%). The same parameters used to model the oxidation of the resin char for the composite also describe well the first reaction zone of the residue. In this case, results show that the volatiles released from the oxidation of the resin char amount to 23%, a relatively small quantity that is in agreement with the visual appearance of the sample as shown by the SEM pictures (Fig. 8E–F).

The analysis of the thermogravimetric measurements indicates that, for the composite material, the oxidation of the carbon fibres is much slower than that observed and predicted for the residue. It can be understood that the significant amount of glass fibres (about half of the total sample mass in the final reaction stage), which are absent from the residue, hinders the oxygen access to the carbon reaction sites. In this way the process is not any longer controlled by chemical kinetics but by the slower rate of oxygen diffusion. Hence, the kinetics for the oxidation of the carbon fibres are evaluated from the curves of the residue which, as anticipated, is free from the glass fibres. This presents a high well defined peak for a temperature of approximately 875 K (as for the curve of the composite material), which is very well (deviations of 1–1.5%) described by an activation energy of 185 kJ/mol, a value typically reported for pure carbon and carbonaceous material oxidation [22].

It is not possible to compare the oxidation kinetics of the carbon/glass reinforced cyanate ester composite under study with previous findings as the literature on this topic is scarce. A previous investigation [14] about the decomposition in inert atmosphere (versus the air of this study) of nine cyanate ester monomers with different chemical structure, by means of thermogravimetry, solid-state and volatile product analysis, shows that in all cases the reaction begins with hydrocarbon chain scission and cross-linking at temperatures between 673–723 K with negligible mass loss. It is always followed by decyclization of the triazine ring at 723 K that liberates volatile cyanate ester decomposition products with a primary solid residue (this is the major step for all the monomers). Subsequently, at about 773–1023 K, the decomposition of the primary residue takes place with the elimination of alkenes and hydrogen leaving a secondary carbonaceous char containing residual oxygen and nitrogen. It is also reported [14], based on literature results, that the decomposition mechanism in air is different as it proceeds via rapid hydrolysis of the ether oxygen bond between the phenyl and triazine rings at temperatures of 623–693 K in the presence of moisture, a result that agrees well with the results of this study (the maximum devolatilization rate for the oxidative decomposition step is around 650 K). Finally, from the results of the kinetic analysis, it can also be understood that, in the oxidation of thermally thick samples, the induction stage may be partly attributed to the low-temperature oxidation of the resin char.

4. Conclusions

The decomposition and oxidation characteristics have been investigated of a commercial composite consisting of carbon and glass fibres impregnated with a thermosetting resin based on polymerized aromatic cyanate ester compounds. A first set of experiments has been carried out for thermally thick samples exposed in a chamber, preheated at 650–950 K, under a continuous gas flow rate (inlet air or nitrogen velocity of 0.6–4.2 cm/s or 0.6 cm/s, respectively). Temperature measurements were used to evaluate the characteristic times and temperatures of the process. An initial inert stage is always observed, when the maximum heating rate is achieved (9–26 K/s). This presents a linear increase with the heating temperature and is almost independent of the gas flow rate. Then, in the presence of air, three main stages have been observed corresponding to oxidative decomposition of the polymeric resin (temperatures between 503–680 K) followed by the heterogeneous processes of solid ignition delay and oxidation with maximum temperatures up to 670–1100 K. The duration of the oxidative decomposition stage is always much shorter than that of the oxidation stages (factors of 60–85). It is significantly affected by the heating temperature (the characteristic times are roughly halved for heating temperatures between 700–950 K) but practically independent of the air gas flow rate. On the other hand, for low air flow rates, variations in the heating temperatures in the same range only cause a small decrease (factors of about 1.3) in the total oxidation times. For high heating temperatures (900 K), an increase in the air flow rate from 0.6 to 4.2 cm/s approximately reduces the total oxidation times of 1.7. These findings support the existence of a mixed kinetic-diffusive control for the heterogeneous oxidation reactions. Moreover, it can be speculated that heterogeneous ignition may concern the entire sample surface (single ignition zone) or may occur at specific surface locations (distributed ignition zones), depending on the heating and flow conditions.

As expected, in nitrogen, the energetics of the conversion process are barely evident. However, results of these experiments demonstrate that the formation of the resin char is influenced by the heating temperature (yields between 67.5 and 42% on resin mass basis). SEM pictures indicate that, contrary to the unreacted composite, the reinforcing fibres are only partially covered by the char formed from the thermal decomposition. The same qualitative features are also shown by the residues collected from the oxidation experiments carried out at low heating temperatures, although the yields of resin char are always lower. In this case, for the more severe thermal conditions, not only the carbon fibres are oxidized but the surface of the glass fibres is also damaged.

Finally, based on thermogravimetric measurements in air of the composite and a residue from a low-temperature oxidation experiment, an oxidation mechanism is developed consisting of three reactions for the oxidative decomposition of the polymeric resin, the oxidation of the resin char and the oxidation of the carbon fibres. Apart from an Arrhenius dependence on temperature, the reaction rates present a power law dependence on the solid mass

fraction. Kinetic parameters have been estimated leading, in particular, to activation energies of 95 kJ/mol (oxidative decomposition of the resin), 136 kJ/mol (oxidation of the resin char) and 185 kJ/mol (oxidation of the carbon fibres).

Acknowledgments

This work is part of the activities carried out in the framework of the project PIROS "Progettazione integrata di componenti multifunzionali per applicazioni in sistemi del settore ferrotranviario e dei vettori di medie dimensioni, associata alla realizzazione di speciali facilities per prove e qualificazioni di materiali in condizioni di fiamma", coordinated by IMAST and funded by the Italian Ministry of Instruction, University and Research (MIUR), the partial support of which is gratefully acknowledged. Thanks are also due to Mr. Sabato Russo of Istituto di Ricerche sulla Combustione, CNR (Napoli, IT), for the SEM photographs.

References

[1] Mouritz AP, Gibson AG. Fire properties of polymer composite materials.. Dordrecht: Springer; 2006.
[2] Mouritz AP, Mathys Z, Gardiner CP. Thermomechanical modelling the fire properties of fibre–polymer composites. Comp Part B 2004;35:467–74.
[3] Bai Y, Vallee T, Keller T. Modelling of thermo-physical properties for FRP composites under elevated and high temperature. Compos Sci Technol 2007;67:3098–109.
[4] Florio J, Henderson JB, Test FL, Hariharan R. A study of the effects of the assumption of local-thermal equilibrium on the overall thermally-induced response of a decomposing, glass-filled polymer composite. Int J Heat Mass Tran 1991;34:135–47.
[5] Di Blasi C, Wichman IS. Effects of solid phase properties on flames spreading over composite materials. Combust Flame 1995;102:229–40.
[6] Nelson MI, Brindley J, McIntosh AC. Ignition of thermally thin thermoplastics – the effectiveness of inert additives in reducing flammability. Polym Degrad Stab 1996;54:255–66.
[7] Staggs JEJ. Modelling the effect of solid-phase additives on thermal degradation of solids. Polym Degrad Stab 1999;64:369–77.
[8] Di Blasi C, Branca C. A mathematical model for the non-steady decomposition of intumescent coatings. AIChE J 2001;47:2359–70.
[9] Neininger SM, Staggs JEJ, Horrock AR, Hill NJ. A study of the global kinetics of thermal degradation of a fibre-intumescent mixture. Polym Degrad Stab 2002; 77:187–94.
[10] Staggs JEJ. Heat and mass transport in developing chars. Polym Degrad Stab 2003;82:297–307.
[11] http://code.google.com/p/gpyro
[12] Galgano A, Di Blasi C, Branca C, Milella E. Thermal response to fire of a fibre reinforced sandwich panel: model formulation, selection of intrinsic properties and experimental validation. Polym Degrad Stab 2009;94:1267–80.
[13] Ramirez ML, Walters R, Lyon RE, Savitski EP. Thermal decomposition of cyanate ester resins. Polym Degrad Stab 2002;78:73–82.
[14] Lyon RE, Walters RN, Gandhi S. Combustibility of cyanate ester resin. Fire Mater 2006;2006(30):89–106.
[15] Branca C, Di Blasi C, Horacek H. Analysis of the combustion kinetics and the thermal behaviour of an intumescent system. Ind Eng Chem Res 2002;41: 2104–14.
[16] Di Blasi C, Branca C. Temperatures of wood particles in a hot-sand bed fluidized by nitrogen. Energy & Fuels 2003;17:247–54.
[17] Branca C, Di Blasi C. Devolatilization and combustion kinetics of wood chars. Energ Fuel 2003;17:1609–15.
[18] Branca C, Di Blasi C, Casu A, Morone V, Costa C. Reaction kinetics and morphological changes of a rigid polyurethane foam during combustion. Thermochim Acta 2003;399:127–37.
[19] Branca C, Di Blasi C. Oxidation characteristics of chars generated from wood impregnated with (NH4)2HPO4 and (NH4)2SO4. Thermochim Acta 2007;456: 120–7.
[20] Branca C, Di Blasi C. Oxidative devolatilization kinetics of wood impregnated with two ammonium salts. Fire Saf J 2008;43:317–24.
[21] Di Blasi C. Modelling chemical and physical processes of wood and biomass pyrolysis. Prog Energ Combust 2008;34:47–90.
[22] Di Blasi C. Combustion and gasification rates of lignocellulosic chars. Prog Energ Combust 2009;35:121–40.